Nuclear Instruments and Methods in Physics Research A 662 (2012) S164–S167

Contents lists available at ScienceDirect

Nuclear Instruments and Methods in Physics Research A

journal homepage: www.elsevier.com/locate/nima

REAS3: A revised implementation of the geosynchrotron model for radio emission from air showers

M. Ludwig [a,*], T. Huege [b]

[a] Karlsruher Institut für Technologie, Institut für Experimentelle Kernphysik, Campus Süd, 76128 Karlsruhe, Germany
[b] Karlsruher Institut für Technologie, Institut für Kernphysik, Campus Nord, 76021 Karlsruhe, Germany

ARTICLE INFO

Available online 5 November 2010

Keywords:
Radio emission
Extensive air showers
Modelling and simulation
Endpoint contribution
Geosynchrotron model

ABSTRACT

Over the past years, the freely available Monte Carlo-code REAS which simulates radio emission from air showers based on the geosynchrotron model, was used regularly for comparisons with data. However, it emerged that in the previous version of the code, emission due to the variation of the number of charged particles within an air shower was not taken into account. In the following article, we show the implementation of these emission contributions in REAS3 by the inclusion of "end-point contributions" and discuss the changes on the predictions of REAS obtained by this revision. The basis for describing radiation processes is an universal description which is gained by the use of the end-point formulation. Hence, not only pure geomagnetic radiation is simulated with REAS3 but also radiation due to the variation of the net charge excess in the air shower, independent of the Earth's magnetic field. Furthermore, we present a comparison of lateral distributions of LOPES data with REAS3-simulated distributions. The comparison shows a good agreement between both, data and REAS3 simulations.

1. Introduction

In recent years, radio detection of cosmic ray air showers has been developed further. With radio detector arrays like LOPES [1,2] and CODALEMA [3,4], correlations of the radio signal with air shower parameters are studied and the dominance of the geomagnetic emission contribution was verified. To study the physics of cosmic rays using radio signals, detailed theoretical simulations are needed. Many approaches for the modelling of radio emission exist, but presently, there are two major approaches, both of which are based on geomagnetic effects [5]. On the one hand the geosynchrotron model as implemented in REAS developed by Huege et al. [6–9], and on the other hand the macroscopic geomagnetic radiation model (MGMR) of Scholten, Werner and Rusydi [10,11]. So far, the two models made conflicting predictions for the radio emission of cosmic ray air showers. Essentially, this could be seen in the different pulse shapes (unipolar for REAS2 and bipolar for MGMR) and the differences in the frequency spectra for low frequencies (dropping to zero for MGMR and levelling off for REAS2). The details of these differences and a comparison of both models are discussed in Ref. [12]. It arose that in REAS2, radiation due to the variation of the number of charged particles in EAS was not considered as it is the case for nearly all time-domain approaches as well. The reason for this missing contribution was a flaw in the implementation of the radiation process of the geosynchrotron radiation. In REAS3 [13], this flaw was solved. In the following sections, the details of the implementation as well as the results are illustrated.

2. General functionality of REAS

To understand what was missing in the techincal implementation of radio emission in REAS2 it is helpful to know the general structure of this Monte Carlo-code. First, the air shower is simulated with CORSIKA [14] saving all important information, e.g. the distribution of energy and momentum of the particles, in histograms. On the basis of these histograms, in REAS, shower particles are generated according to the desired distributions derived with CORSIKA. In the simulation code, each particle is followed analytically on its track through the Earth's magnetic field. Note that the real particle trajectories are described by several unrelated short tracks. Finally, the radiation given from all shower particles is superposed for each single observer position. In REAS2, only radiation processes along the trajectories were treated, but not at the end or the beginning of the tracks. This can be compared with a situation that the particles arrive with velocity $v \approx c$ given by CORSIKA, enter the Earth's magnetic field where they are deflected on a short curved track and finally fly out of the influence of the geomagnetic field with velocity $v \approx c$ (cf. left sketch of Fig. 1). To revise the flaw in the derivation of the radiation process of the geosynchrotron radiation, emission contributions at the beginning and the end of the tracks have to be taken into account, i.e. radiation due to the acceleration of the particle at the starting point of the

* Corresponding author.
E-mail address: marianne.ludwig@kit.edu (M. Ludwig).

0168-9002/$ - see front matter © 2010 Elsevier B.V. All rights reserved.
doi:10.1016/j.nima.2010.10.115

trajectory and vice-versa deceleration of the particle at the stopping point is considered. To implement this radiation, the best description of the radiation processes is an end-point formulation [15]. In this case, the tracks are described by straight track segments joined by "kinks" (cf. right sketch of Fig. 1). If at a given atmospheric depth more particle trajectories start than end, e.g. the number of particle declines, this results in a net contribution. (An equivalent approach for dense media is done in Ref. [19].)

3. Incorporation of end-point contributions

Adding the discrete end-point contributions to the continuous contributions along the tracks may produce problems, e.g., there is a risk of double-counting. To get a consistent description of all radiation processes in the simulation, it is convenient to use the end-point formulation throughout. Radiation occurs if the velocity of the particle changes, i.e., in a kink of the track. Because the change of the velocity can be considered instantaneous with respect to the times of interest ($\delta t \ll 1/\nu_{\mathrm{observed}}$ and $\nu_{\mathrm{observed}} \leq 100-1000$ MHz) only the time-averaged process is of interest. Hence, the time-integrated field strength of the radiation formula can be calculated. Eq. (1) shows the result for the radiation in one kink of the track,

$$\int \vec{E}(\vec{x},t)\,dt = \int_{t_1}^{t_2} \frac{e}{c} \left| \frac{\vec{n} \times [(\vec{n}-\vec{\beta}) \times \dot{\vec{\beta}}]}{(1-\vec{\beta}\cdot\vec{n})^3 R} \right|_{ret} \mathrm{d}t = \vec{F}(t_2) - \vec{F}(t_1)$$
$$= \frac{e}{cR}\left(\frac{\vec{n}\times(\vec{n}\times\vec{\beta}_2)}{(1-\vec{\beta}_2\vec{n})}\right) - \frac{e}{cR}\left(\frac{\vec{n}\times(\vec{n}\times\vec{\beta}_1)}{(1-\vec{\beta}_1\vec{n})}\right) \quad (1)$$

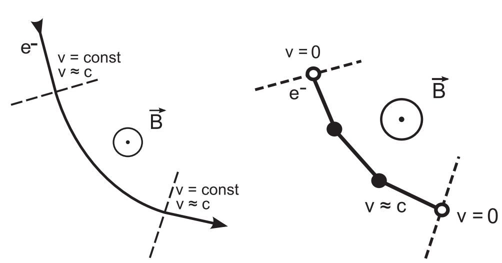

Fig. 1. Sketch of the trajectories how they are implemented in REAS. Left: REAS2 and right: REAS3.

where e indicates the particle charge, $\vec{\beta} = \vec{v}(t)/c$ is given by the particle velocity, $R(t) = |\vec{R}(t)|$ describes the vector between particle and observer position and $\vec{n}(t) = \vec{R}(t)/R(t)$ is the line-of-sight direction between particle and observer. The index "ret" means that the equation needs to be evaluated in retarded time. $\vec{\beta}_1$ corresponds to the velocity before and $\vec{\beta}_2$ to the velocity after the kink. In this completely universal (cf. Ref. [15]) and discrete calculation, radiation at the end or the beginning of the track corresponds to kinks where one velocity is equivalent to zero, i.e., one term of the integrated sum vanishes.

4. Results

4.1. Comparison between REAS2 and REAS3

In this section, a short overview about the major changes from REAS2 to REAS3 is given. In Ref. [13] more details and discussion can be found. For the comparison, several simulations were done with a set of prototype showers. For this article, a simple shower geometry is chosen where the geomganetic angle is 90°, i.e., a vertical shower with a primary energy of 10^{17} eV and a horizontal magnetic field of 0.23 G was selected. Since one typical shower out of many CORSIKA simulated air showers was chosen, shower-to-shower fluctuations do not influence this comparison. For REAS2 and REAS3 the same CORSIKA shower was taken as the basis. In Fig. 2 the raw pulses of REAS2 and REAS3 for an observer 100 m north of the shower core are shown as well as the frequency spectra for observers 100 m north and east of the shower core. It is obvious that the pulse shape changed from unipolar to bipolar. This change agrees with the theoretical expectation since the source of the radio emission exists only over a finite time in a finite region of space (cf. Ref. [16]). In the frequency spectra (right plot of Fig. 2) this behaviour can be seen as well because the spectral field strengths drop to zero for frequency zero. In addition, the spectral field strength for observers at different azimuthal positions differs less in REAS3 than in REAS2, which indicates an increased azimuthal symmetry of REAS3 compared to REAS2. For the spectra of Fig. 2 one observer in the north and in the east of the shower core is selected. In general, the spectra got flatter for REAS3. The increased azimuthal symmetry is again visible in the contour plots of Fig. 3 for the total field strength which gives an overall impression of the changes from REAS2 to REAS3. In the contour plot of REAS3, an east-west asymmetry is distinguishable, i.e., the signal in the

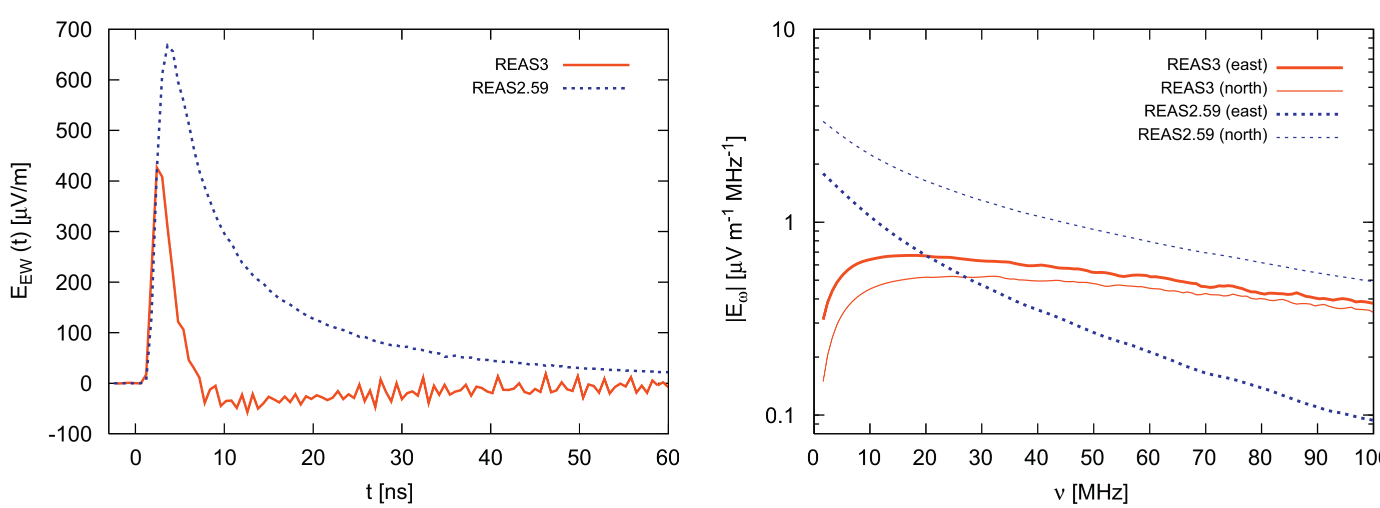

Fig. 2. Direct comparison of REAS2 (dashed blue) and REAS3 (solid red) for a vertical air shower and observer distance of 100 m. Left: Raw pulse for an observer 100m north of the shower core. Right: Frequency spectra for observers east (thick lines) and north (thin lines) of the shower core. (For interpretation of the references to color in this figure legend, the reader is referred to the web version of this article.)